

An Evaluation of Image Sampling and Compression for Human Iris Recognition

Soumyadip Rakshit, *Student Member, IEEE*, and Donald M. Monro, *Member, IEEE*

Abstract—The resilience of identity verification systems to subsampling and compression of human iris images is investigated for three high-performance iris-matching algorithms. For evaluation, 2156 images from 308 irises from the extended Chinese Academy of Sciences Institute of Automation database were mapped into a rectangular format with 512 pixels circumferentially and 80 radially. For identity verification, the 48 rows that were closest to the pupil were taken and images were resized by subsampling their Fourier coefficients. Negligible degradation in verification is observed if at least 171 circumferential and 16 radial Fourier coefficients are preserved, which would correspond to sampling the polar image at 342×32 pixels. With JPEG2000 compression, improved matching performance is observed down to 0.3 b/pixel (bpp), attributed to noise reduction without a significant loss of texture. To ensure that the iris-matching algorithms studied are not degraded by image compression, it is recommended that normalized iris images should be exchanged at 512×80 pixel resolution, compressed by JPEG 2000 to 0.5 bpp. This achieves a smaller file size than the ANSI/INCITS 379-2004 iris image interchange format.

Index Terms—Biometrics, compression, iris recognition, spectral analysis, subsampling.

I. INTRODUCTION

BIOMETRICS-BASED human authentication systems [1]–[8] are becoming more important as governments and corporations worldwide deploy them in such schemes as access and border control, time and attendance, driving license registration, and national ID cards schemes [9]–[11]. To design and implement robust systems capable of mass deployment, one needs to address key issues, such as human factors, environmental conditions, system interoperability, and image standards. Additionally, the requirement for collection, storage, and sharing of large volumes of data calls for compression at the point of capture to reduce the bandwidth requirements for exchanging data with other parts of the system [12], [13].

The iris is a strong contender alongside face and fingerprints for inclusion in multimodal recognition systems [14], [15]. Interest in the field of coding of iris images for recognition originated with Daugman's system using Gabor wavelets [16]–[19] that were patented in 1994 [20]. Other previous work was done by Wildes [21] and Boles [22]. More recently, with the expiry

Manuscript received September 21, 2006; revised April 10, 2007. This work was sponsored by Smart Sensors Ltd., Bristol, U.K. The associate editor coordinating the review of this manuscript and approving it for publication was Prof. Vijaya Kumar Bhagavatula.

The authors are with the Department of Electronic and Electrical Engineering, University of Bath, Bath BA2 7AY, U.K. (e-mail: S.Rakshit@bath.ac.uk; D.M.Monro@bath.ac.uk).

Color versions of one or more of the figures in this paper are available online at <http://ieeexplore.ieee.org>.

Digital Object Identifier 10.1109/TIFS.2007.902401

of key patents in this area, renewed interest has been expressed by various commercial and government organizations in finding alternative solutions and carrying out detailed studies. This has led to a surge in recent activity leading to improved solutions for image capture, quality assessment, preprocessing, feature extraction, and matching [23]–[47].

Among the various lossless compression algorithms available today, achievable compression is of the order of 1.5:1 to 3:1. Alternatively, lossy codecs can compress images further with varying degrees of loss. JPEG2000 is a relatively new compression standard published by the Joint Photographic Experts Group [48], [49]. Its use of wavelet technology results in efficiently compressed images with lower error rates than with previous image compression technologies [50], [51]. A high-quality standard compression algorithm, such as JPEG2000, would provide an open system for exchanging iris images.

Normalized iris image subsampling and compression and the effect on system performance have not been previously reported. This paper studies the sampling requirements for reliable identity verification using human iris images, and evaluates the effect of data compression on the performance of three state-of-the-art verification algorithms. The rest of this paper is organized as follows. An overview of the iris recognition algorithms considered is given in Section II along with a brief synopsis of the preprocessing steps involved. Section III studies the sampling requirements for reliable identity verification from the point of view of frequency-domain processing. The effects of JPEG2000 compression on normalized iris images and verification performance are investigated in Section IV. Finally, conclusions are drawn and sampling recommendations for the interchange of iris images are made in Section V.

II. BACKGROUND

A brief summary of the recognition algorithms developed by Daugman, Tan, and Monro follows. In Daugman's method, the iris image is filtered using a family of multiscale Gabor filters [16], [17]. The phase structure is then demodulated into a sequence of complex-valued phasors which are projected onto a four-quadrant complex plane to generate a binary iris code. Two implementations of the Daugman algorithm were used in our studies. Ma of the Chinese Academy of Sciences Institute of Automation (CASIA) provided us with his implementation of the Daugman algorithm, where he optimized the Gabor parameters for the CASIA dataset. The other implementation was based on Masek's publicly available Matlab source code [33]. Both implementations performed similarly in our study, as the results will show.

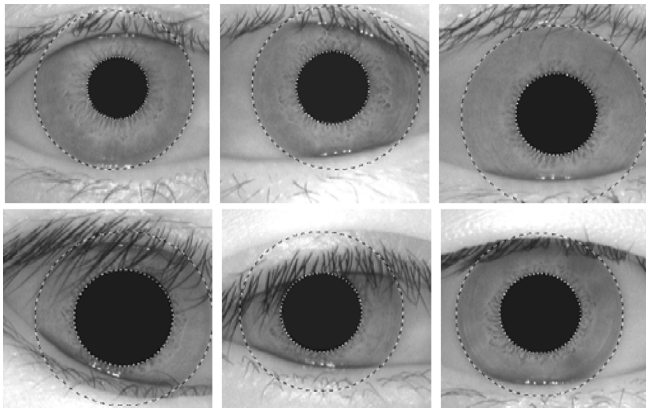


Fig. 1. Sample localized images from the CASIA database.

Tan generates a bank of 1-D intensity signals from the iris images [44]. These are then filtered with the help of a special class of wavelets and the position of local sharp variations is recorded to form the feature vector. This algorithm was obtained from Tan of CASIA, as used in [56]. For the Monro iris transform (MIT), the image is first divided into angular rectangular patches of size 8×12 with each patch overlapping the next one by 50% [46]. These fragments are then averaged across their width to form 1-D vectors in an attempt to reduce noise and lower complexity. A 1/4th Hanning Window is then applied to the vectors followed by the fast Fourier transform (FFT) to obtain frequency-domain coefficients with reduced spectral leakage. The frequency magnitude difference between adjacent patches is then calculated and a binary feature vector is obtained from the zero crossings of each difference. For matching, a nearest neighbor approach is taken, with the distance criteria being the Hamming distance between the feature vectors.

Common to all three algorithms is the preprocessing stage of iris localization and normalization into a rectangular image prior to coding, which is summarized here. The location of the pupil and outer iris boundaries begins with the removal of the bright spot in the pupil caused by the reflection of the infrared light source. This reduces the influence of the high gray-level values on the grayscale distribution. Then, the image is scanned to isolate a region containing the pupil and iris. This is accomplished by a heuristic method based on the assumption that the majority of image rows and columns passing through the pupil will have a larger gray-level variance than those not passing through the pupil. It is assumed that the pupil is circular and because the pupil boundary is a distinct edge feature, a Hough transform is used to find the center and radius of the pupil. To locate the outer boundary of the iris (limbus), a horizontal line through the pupil center is scanned for the jumps in the gray level on either side of the pupil. The limbus is normally circular but its center does not necessarily coincide with that of the pupil. Some examples of localized images from the CASIA database are shown in Fig. 1.

Due to the dilation and constriction of the human pupil, the radial size of the iris varies under different illumination conditions and is in response to physiological factors. It is widely accepted that the resulting deformation of the iris texture can be approximated as a linear deformation [52], [53]. Once the iris boundaries are known, a rectangular image array can be

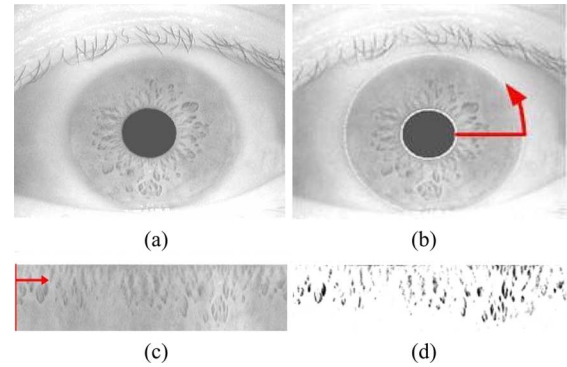


Fig. 2. (a) Typical human eye image. (b) Iris outlines detected. (c) Resampled: polar—Cartesian. (d) Intensity enhanced.

mapped to an angular and radial position in the iris. This position will not, in general, map exactly onto a pixel in the source image, so the normalized gray value is obtained by bilinear interpolation from its four nearest neighbors. Finally, the gray levels are adjusted by removing the peak illumination caused by light sources reflecting from the eye, estimating and subtracting the slowly varying background illumination, and equalizing the gray-level histogram of the iris image. The final normalized image is of resolution 512 by 80, from which we code only the 48 rows closest to the pupil to mitigate the effect of eyelids. Fig. 2 illustrates a typical result of this process.

III. FREQUENCY CONTENT AND SUBSAMPLING

As is evident from casual observation, iris images have a higher frequency content circumferentially than they have radially. As a preliminary indication of the relative requirements of circumferential and radial sampling, spectral analysis by a 1-D FFT in both directions was carried out. Due to the data being naturally periodic in the circumferential direction, no horizontal windowing was required of the normalized images. For radial (vertical) sampling, a 1/8th tapered cosine window was used at each end of each column of pixels prior to spectral analysis. Fig. 3(a) shows the average normalized power spectrum taken over 512 columns for 2156 images. The normalized ac power spectrum averaged over all 48 rows is shown in Fig. 3(b). It is clear that the requirements for circumferential sampling are much higher than for radial sampling. For example, 99% of the averaged image power is contained within 143 coefficients circumferentially and 8 radially. It will be shown that more than 99% of the image power must be preserved so that the verification performance of the three systems that are studied is not degraded.

To evaluate the sampling requirements, 2156 normalized iris images of 308 eyes were taken from the CASIA database [54]. These were then subsampled to various degrees in an attempt to simulate low-resolution image capture and observe the effects of high-frequency content on system performance. Both spatial- and frequency-domain approaches were used. In the spatial case, multiple pixels were replaced by their mean gray level. This method, applied in both directions, is suitable for simulating low-resolution charge-coupled device (CCD) devices, but is restricted to integer subsamplings. The normalized image of size 512×48 was subsampled to 256, 128, and 64 columns, and

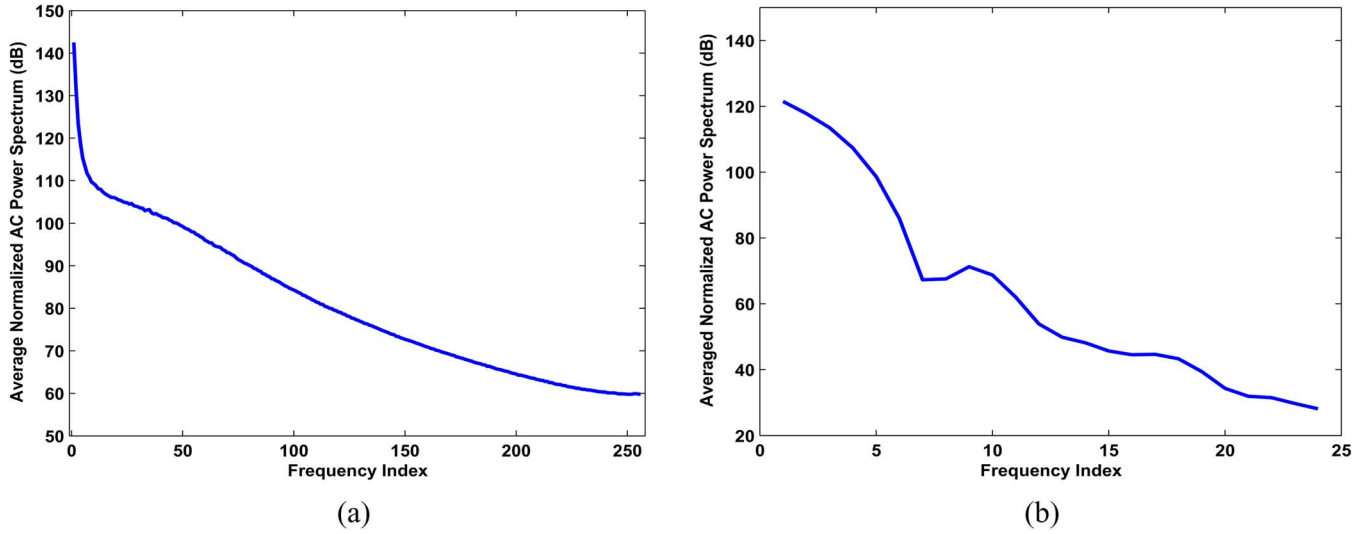


Fig. 3. Average normalized ac power spectrum in the (a) circumferential and (b) radial direction of normalized iris images.

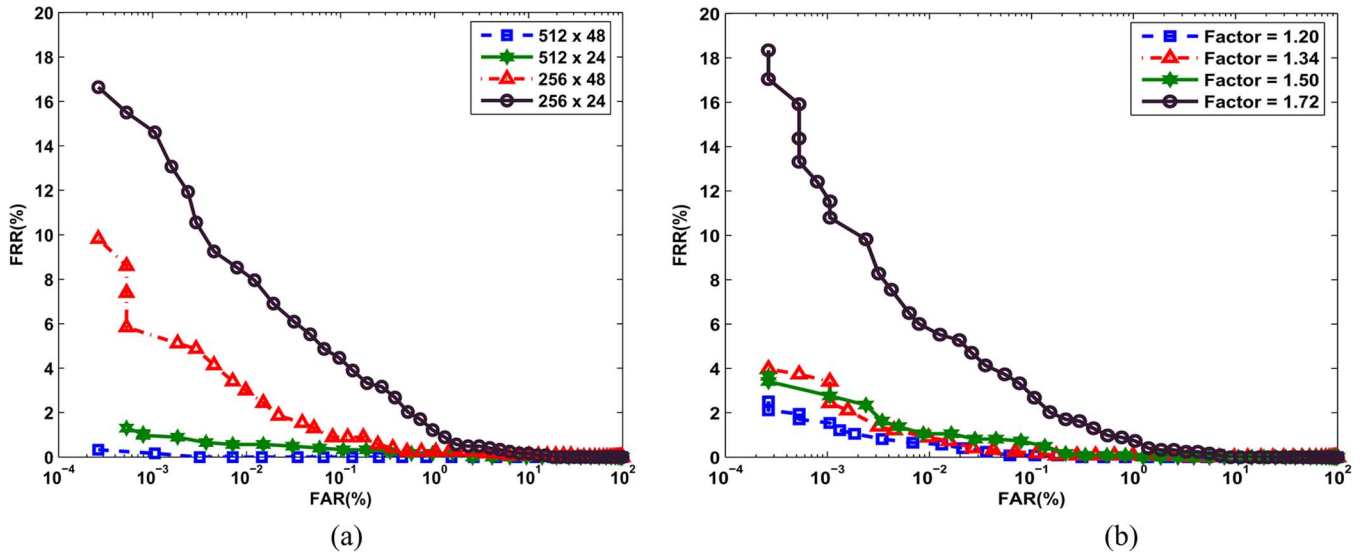


Fig. 4. Effects of subsampling on the MIT ROC curve for various factors and resolutions in (a) spatial and (b) frequency domain.

24, 16, and 8 rows. All combinations were explored and, as expected, the results showed degradation in system performance in all cases.

The receiver operating characteristic (ROC) curves, obtained by plotting the false rejection rates (FRR) against the false acceptance rates (FAR) is shown in Fig. 4(a) for some resolutions. For the same downsampling ratios, the performance degradations are more pronounced in the circumferential direction than in the radial one. For example, column subsampling by a factor of 4 increases the false reject to 97.5% at a false accept of 0.001%. On the other hand, the same subsampling ratio, when applied to the rows, results in an FRR of 17.5% FRR at the same levels of FAR. Since downsampling by the minimum factor of 2 is already too severe, it is necessary to examine noninteger downsampling ratios between 1 and 2. This can be achieved by using the Fourier domain methods of decimation.

In the second method, the inverse Fourier transform of a reduced frequency domain was used to generate subsampled

images. The effect of subsampling-induced aliasing was simulated by overlapping the symmetrical high-frequency regions and adding them prior to truncation. Fig. 5(a) shows the symmetrical power spectrum of the first column of a normalized iris image, where the shaded region indicates the aliasing overlap. In order to eliminate frequencies above a certain value, say X , overlapping must be performed equally on either side of X up to the midfrequency. As can be seen from Fig. 5(b), this method can be extended to two dimensions by considering conjugate symmetry and applying superimposition in both directions.

In the experiments, the circumferential and radial directions of the 48 by 512 iris region were subsampled by the same factors to preserve the aspect ratio, over the range from 1.20 to 4.00, corresponding to numbers of radial pixels from 40 down to 12 in steps of 4. From Fig. 4(b), we see that acceptable system performance is preserved up to a factor of 1.50, where the size of the central iris region is reduced from 48×512 pixels to 32×342 . The total image power retained compared to the original image

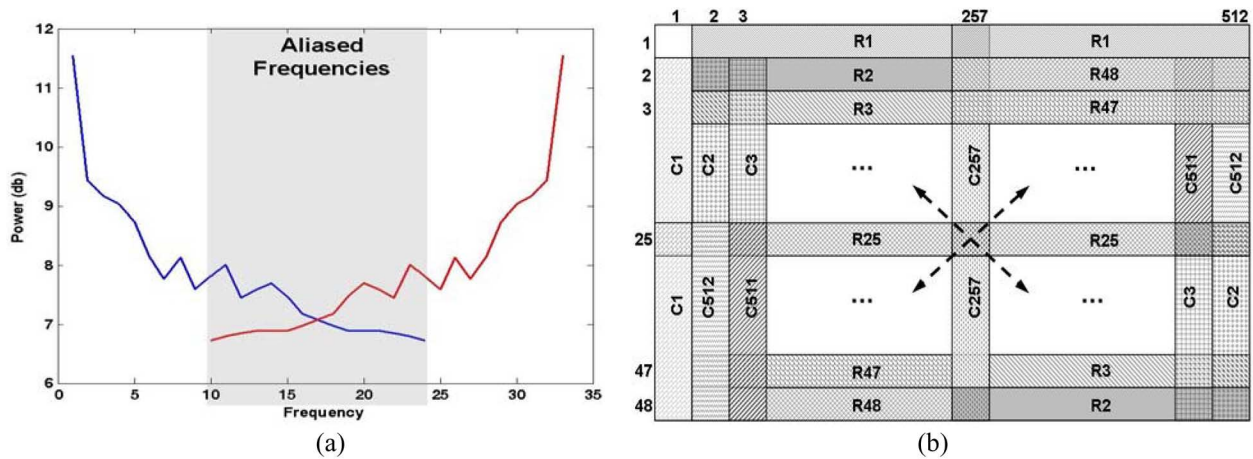


Fig. 5. (a) Symmetrical power spectrum of the first column of a normalized iris image. (b) Fourier symmetry in 2-D FFT.

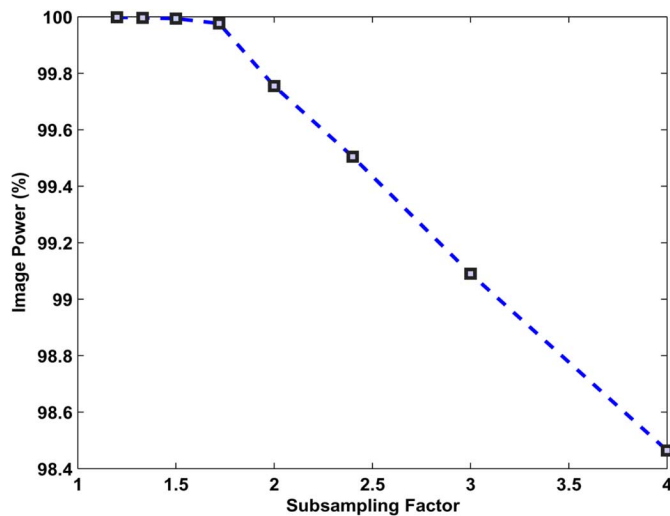


Fig. 6. Effects of subsampling on the image power for all factors studied.

is shown in Fig. 6, and is 99.994% at the acceptable subsampling factor of 1.50. These results show that a minimum of 16 complex radial Fourier coefficients and 171 circumferential ones are required in the frequency domain to describe the central iris region. For higher subsampling ratios, the ROCs degrade beyond practical use. The use of low-resolution sensors for image acquisition could thus prove to be a major hindrance in achieving acceptable error rates and the same applies to excessive downsampling. As will be shown later, JPEG2000 compression produces far better results with significantly lower memory requirements.

IV. COMPRESSION BY JPEG2000

To evaluate the effect of compression on iris images, the JPEG 2000 codec Kakadu Version 4.3 was used to compress and decompress all normalized irises in the database [55]. The use of wavelet technology in JPEG2000 results in more efficiently compressed images with lower error rates than with previous image compression technology [50], [51]. The compression experiment was carried out over a range of bit-rates between 0.1 b/pixel (bpp), where significant degradation is expected, to 1 bpp, where images are widely accepted to be

visually lossless. As the compression was carried out from 1.0 bpp downwards, it was observed that despite an overall smoothing effect, the essential iris texture was retained to as low as 0.3 bpp. Beyond that, the loss in texture detail is significant and at 0.1 bpp, the image is blurred beyond recognition. Sample images compressed at 1.0, 0.5, and 0.1 bpp are shown in Fig. 7 in order to demonstrate this effect.

Various image compression effects were studied and the results obtained agreed with expectations. Plots of entropy, correlation, and peak-to-signal noise ratio (PSNR) showed a gradual decrease with an increase in compression ratios up to 0.2 bpp, after which the drop was significantly more pronounced. Maximum RMSE, a measure of the maximum difference in the gray level between original and compressed images, showed a similar response in the reverse direction. PSNR and maximum root mean square error (RMSE) plots averaged over all images for the range of compressions studied are shown in Fig. 8.

The spectral analysis, carried out for uncompressed images in Section III, was repeated for all compression values. Fig. 9 shows the loss in power of the FFT coefficients over the range of compression rates for circumferential and radial analysis. It is observed that 99% of the power is preserved down to 0.2-bpp compression both circumferentially and radially.

To assess the effect of compression on the performance of the competing algorithms, compressed and expanded images were used as both the registered and matching sets over the range of compression studied. At each compression ratio, three images of each of the 308 eyes were coded into the registered database and the remaining 1232 images were coded and matched against them. The ROC curves generated for all compression rates for the four algorithms reveal interesting results. As the compression ratio increases, the system performance initially improves up to 0.5 bpp, where the retained image power is found to be 99.84%. This result can be explained as being the consequence of image denoising by the compression process, in which moderate compression produces better performance curves due to noise removal without damaging the image texture that is important for matching. The error curves are acceptable up to 0.3 bpp, but beyond that, performance degrades markedly so that at 0.1 bpp, the error rates are too high to be of

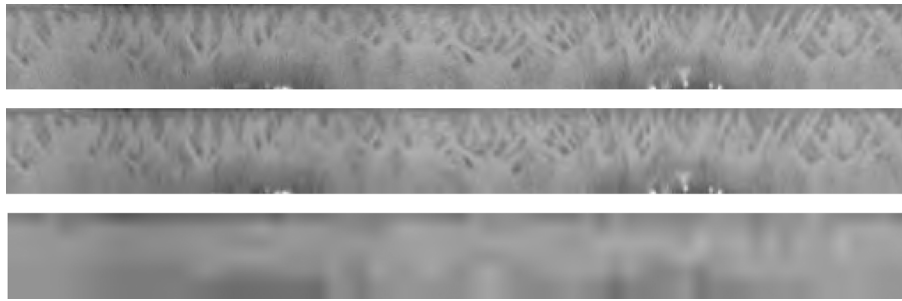


Fig. 7. Normalized iris images compressed at 1.0, 0.5, and 0.1 bpp.

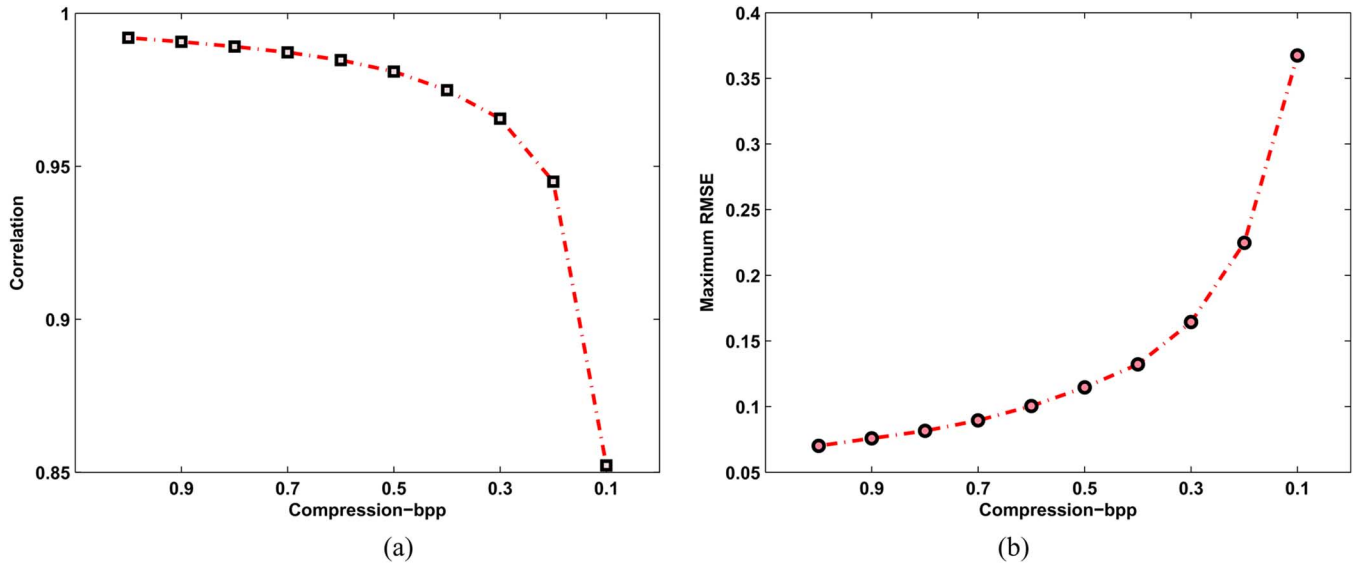


Fig. 8. Effect of compression on image quality. (a) Correlation. (b) Maximum RMSE.

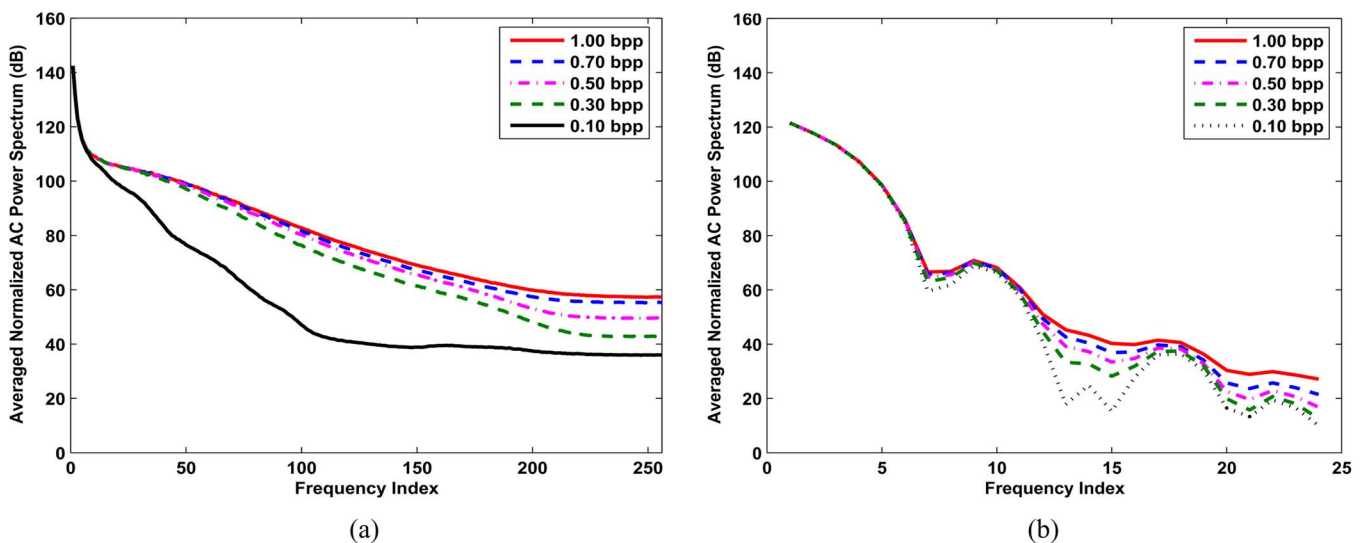


Fig. 9. Average normalized ac power spectrum for various compression rates in (a) circumferential and (b) radial direction of normalized images.

any practical use. ROC curve combinations for original images and those compressed at 0.5 bpp are shown in Fig. 10(a) and (b), respectively.

The correct recognition rate (CRR), the ratio of correctly identified subjects to the total population, remains at 100% for all algorithms for bit rates above 0.3 bpp. In our studies, we

have found that a more meaningful indication of where the verification begins to degrade is the FAR at the first rejection. This is the value of the FAR at the point when the first nonzero false reject occurs. It can be obtained by tracing the ROC curve back along the FAR axis until it deviates from it. This indicates the extent to which the matching threshold may be reduced

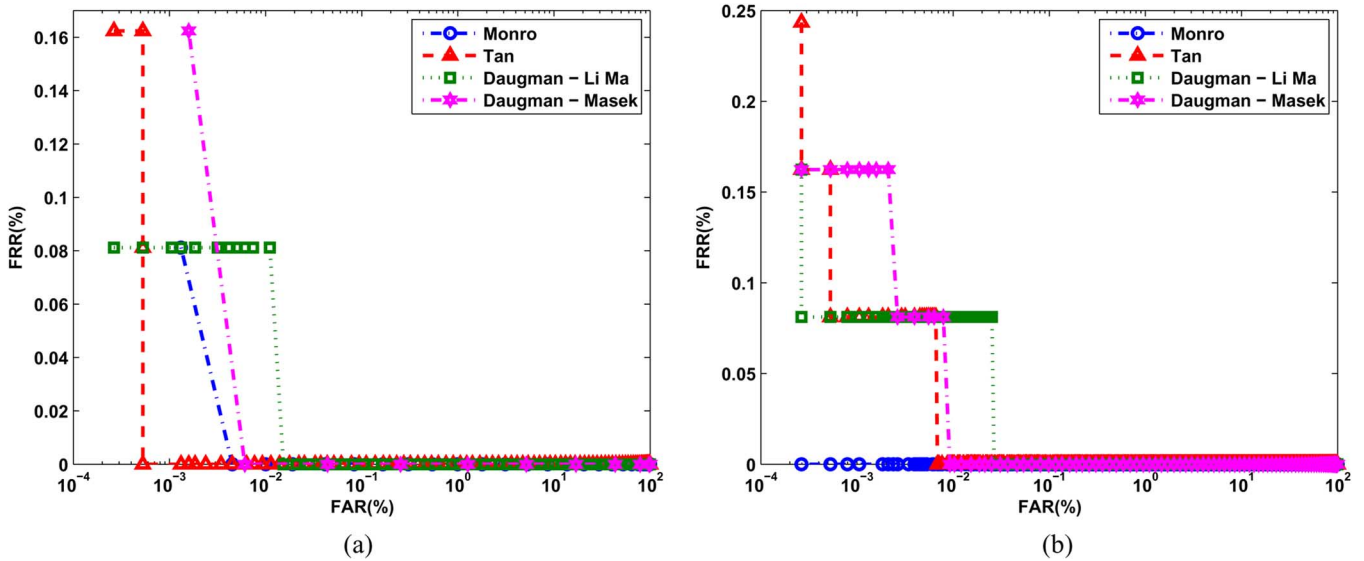


Fig. 10. (a) ROC curves for the four algorithms with original normalized images. (b) Same ROC curves on images compressed by JPEG2000 at 0.5 bpp.

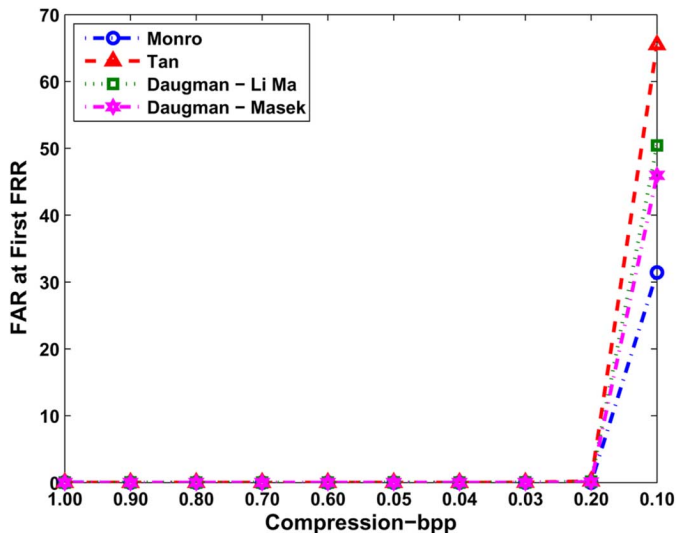


Fig. 11. FAR at first rejection as a function of compression for the four algorithms.

without causing any false rejections for a given data set. A lower value of this threshold is desirable as it keeps the FAR to a minimum. Fig. 11 clearly demonstrates that the degrading effect of compression on this metric comes into effect only from 0.2 bpp downwards.

V. CONCLUSION

The technology of iris coding is still at an early stage, due in no small part to commercial constraints arising from generic patents. It is important that as systems are developed, compared, and improved that any standardized iris format should err on the side of caution in specifying a compaction ratio. The proposed ANSI/INCITS 379-2004 iris image interchange format [57] subsamples a normalized human iris image to 256 circumferential and eight radial pixels [57], [58]. The spectral analysis carried out here suggests that this should preserve 99% of the image power radially and more circumferentially. However,

our subsampling studies suggest that 99% of the power is not sufficient and, therefore, the proposed standard does not provide a level playing field for evaluation of competing methodologies. Our analysis shows that a minimum of 171 Fourier coefficients are required circumferentially and 16 radially to preserve 99.99% of the image power and give acceptable ROC curves. For practical and efficient image processing purposes, it is recommended that the normalized iris image size be fixed at 80 rows and 512 columns.

Moderate compression of normalized iris images, by JPEG2000 to around 0.5bpp, leads to improved ROC curves due to noise removal without detrimental effects on image texture. In light of this finding, it is recommended that JPEG2000 compression at 0.5 bpp be used for the interchange of normalized iris images to allow for the future development of more accurate codes. If required, compression rates as low as 0.3 bpp could be used without degrading the performance significantly.

ACKNOWLEDGMENT

The authors would like to acknowledge Prof. T. Tan, Chinese Academy of Sciences Institute of Automation (CASIA), and Professor M. Smith, Purdue University, for sharing their iris image databases. The authors would also like to thank Dr. L. Ma of CASIA for his implementations in MATLAB of the Tan and Daugman algorithms and Prof. R. Wildes, York University; Dr. D. Taubman, University of New South Wales; Prof. K. Meek, Cardiff University; Prof. J. Marshall, King's College London; and the anonymous reviewers for their valuable comments and suggestions.

REFERENCES

- [1] U. Uludag, S. Pankanti, S. Prabhakar, and A. Jain, "Biometric cryptosystems: Issues and challenges," *Proc. IEEE*, vol. 92, no. 6, pp. 948–960, Jun. 2004.
- [2] A. Ross and A. K. Jain, "Multimodal biometrics: An overview," in *Proc. 12th Eur. Signal Process. Conf.*, 2004, pp. 1221–1224.
- [3] A. K. Jain, A. Ross, and S. Prabhakar, "An introduction to biometric recognition," *IEEE Trans. Circuits Syst. Video Technol.*, vol. 14, no. 1, pp. 4–20, Jan. 2004.

- [4] A. K. Jain, S. Pankanti, S. Prabhakar, L. Hong, A. Ross, and J. L. Wayman, "Biometrics: A grand challenge," in *Proc. 17th Int. Conf. Pattern Recognition*, 2004, vol. 2, pp. 935–942.
- [5] A. K. Jain, L. Hong, and S. Pankanti, "Biometrics: Promising frontiers for emerging identification market," *Commun. ACM*, vol. 43, pp. 91–98, 2000.
- [6] P. S. Aleksic and A. K. Katsaggelos, "Audio-Visual biometrics," *Proc. IEEE*, vol. 94, no. 11, pp. 2025–2044, Nov. 2006.
- [7] A. K. Jain, R. Bolle, and S. Pankanti, *Biometrics: Personal Identification in Networked Society*. Norwell, MA: Kluwer, 1998.
- [8] J. Ortega-Garcia, J. Bigun, D. Reynolds, and J. Gonzalez-Rodriguez, "Authentication gets personal with biometrics," *IEEE Signal Process. Mag.*, vol. 21, no. 2, pp. 50–62, Mar. 2004.
- [9] T. Mansfield and M. Rejman-Greene, "Feasibility study on the use of biometrics in an entitlement scheme," National Phys. Lab., Teddington, U.K., Feb. 2003.
- [10] D. Blunkett, "Identity cards—The next steps," *U.K. Government Home Office Documents*, 2003.
- [11] D. Blunkett, "Identity cards—A summary of findings from the consultation on legislation on identity cards," *U.K. Government Home Office Documents*, 2004.
- [12] J. L. Wayman, "Fundamentals of biometric authentication technologies," *Int. J. Image Graphics*, vol. 1, pp. 93–113, 2001.
- [13] J. L. Wayman, "A generalized biometric identification system model," in *Proc. Conf. Rec. 31st Asilomar Conf. Signals, Syst. Comput.*, 1997, vol. 1, pp. 291–295.
- [14] UK Passport Service Biometrics Enrolment Trial Atos Origin, 2005.
- [15] "Independent testing of iris recognition technology," Final Rep., Int. Biometric Group, 2005.
- [16] J. Daugman, "High confidence visual recognition of persons by a test of statistical independence," *IEEE Trans. Pattern Anal. Mach. Intell.*, vol. 15, no. 11, pp. 1148–1161, Nov. 1993.
- [17] J. Daugman, "Statistical richness of visual phase information: Update on recognizing persons by iris patterns," *Int. J. Comput. Vis.*, vol. 45, pp. 25–38, 2001.
- [18] J. Daugman and C. Downing, "Epigenetic randomness, complexity, and singularity of human iris patterns," *Proc. Roy. Soc. (London) B: Biol. Sci.*, vol. 268, pp. 1737–1740, 2001.
- [19] J. Daugman, "The importance of being random: Statistical principles of iris recognition," *Pattern Recognit.*, vol. 36, pp. 279–291, 2003.
- [20] J. Daugman, "Biometric personal identification system based on iris analysis," U.S. No. 5291560, Mar. 1, 1994.
- [21] R. P. Wildes, "Iris recognition: An emerging biometric technology," *Proc. IEEE*, vol. 85, no. 9, pp. 1348–1363, Sep. 1997.
- [22] W. W. Boles and B. Boashash, "A human identification technique using images of the iris and wavelet transform," *IEEE Trans. Signal Process.*, vol. 46, no. 4, pp. 1185–1188, Apr. 1998.
- [23] W. K. Kong and D. Zhang, "Accurate iris segmentation based on novel reflection and eyelash detection model," in *Proc. Int. Symp. Intelligent Multimedia, Video and Speech Processing*, 2001, pp. 263–266.
- [24] C. Tisse, L. Martin, L. Torres, and M. Robert, "Person identification technique using human iris recognition," in *Proc. 15th Int. Conf. Vision Interface*, 2002, pp. 294–299.
- [25] D. Yingzi, B. Bonney, R. Ives, D. Etter, and R. Schultz, "Analysis of partial iris recognition using a 1D approach," in *Proc. IEEE Int. Conf. Acoustics, Speech, and Signal Processing*, 2005, vol. 2, pp. 961–964.
- [26] B. Bonney, R. Ives, D. Etter, and D. Yingzi, "Iris pattern extraction using bit planes and standard deviations," in *Proc. Conf. Rec. 38th Asilomar Signals, Systems and Computers*, 2004, vol. 1, pp. 582–586.
- [27] R. W. Ives, A. J. Guidry, and D. M. Etter, "Iris recognition using histogram analysis," in *Proc. Conf. Rec. 38th Asilomar Conf. Signals, Systems and Computers*, 2004, vol. 1, pp. 562–566.
- [28] S. Lim, K. Lee, O. Byeon, and T. Kim, "Efficient iris recognition through improvement of feature vector and classifier," *ETRI J.*, vol. 23, pp. 61–70, 2001.
- [29] H. Proença and L. A. Alexandre, "A method for the identification of noisy regions in normalized iris images," in *Proc. Int. Conf. Pattern Recognition*, 2006, vol. 4, pp. 405–408.
- [30] H. Proença and L. A. Alexandre, "Iris segmentation methodology for non-cooperative recognition," *Proc. Inst. Elect. Eng. Vision, Image Signal Process.*, vol. 153, pp. 199–205, 2006.
- [31] K. R. Park and J. Kim, "A real-time focusing algorithm for iris recognition camera," *IEEE Trans. Syst., Man Cybern. C, Appl. Rev.*, vol. 35, no. 3, pp. 441–444, Aug. 2005.
- [32] T. A. Camus and R. Wildes, "Reliable and fast eye finding in close-up images," in *Proc. Int. Conf. Pattern Recognition*, 2002, vol. 1, pp. 389–394.
- [33] L. Masek, "Recognition of human iris patterns for biometric identification," B.E. dissertation, School Comput. Sci. Software Eng., Univ. Western Australia, Perth, Australia, 2003.
- [34] J. Zuo, N. A. Schmid, and X. Chen, "On performance comparison of real and synthetic iris images," in *Proc. IEEE Int. Conf. Image Processing*, Atlanta, GA, Oct. 2006, no. 8–11, pp. 305–308.
- [35] N. A. Schmid, M. Ketkar, H. Singh, and B. Cukic, "Performance analysis of iris-based identification system at the matching score level," *IEEE Trans. Inf. Forensics Security*, vol. 1, no. 2, pp. 154–168, Jun. 2006.
- [36] N. A. Schmid, B. Cukic, M. Ketkar, and H. Singh, "Performance analysis of iris based identification system at the matching score level," in *Proc. Int. Conf. Acoustics, Speech, and Signal Processing*, 2005, vol. 2, pp. 93–96.
- [37] N. D. Kalka, J. Zuo, N. A. Schmid, and B. Cukic, "Image quality assessment for iris biometric," *Proc. SPIE*, vol. 6202, 2006.
- [38] V. Dorairaj, N. A. Schmid, and G. Fahmy, "Performance evaluation of non-ideal iris based recognition system implementing global ICA encoding," in *Proc. Int. Conf. Image Processing*, 2005, vol. 3, pp. 285–258.
- [39] N. A. Schmid and J. A. O'Sullivan, "Performance prediction methodology for biometric systems using a large deviations approach," *IEEE Trans. Signal Process.*, vol. 52, no. 10, pt. 2, pp. 3036–3045, Oct. 2004.
- [40] C. Boyce, A. Ross, M. Monaco, L. Hornak, and L. Xin, "Multispectral iris analysis: A preliminary study," in *Proc. Conf. Computer Vision and Pattern Recognition Workshop*, 2006, pp. 51–59.
- [41] J. Thornton, M. Savvides, and B. V. K. V. Kumar, "Robust iris recognition using advanced correlation techniques," in *Proc. Int. Conf. Image Analysis and Recognition*, 2005, pp. 1098–1105.
- [42] J. Thornton, M. Savvides, and B. V. K. V. Kumar, "Enhanced iris matching using estimation of in-plane nonlinear deformations," presented at the SPIE Defense Security Symp. Biometric Identification Technologies, 2006.
- [43] J. Cui, Y. Wang, J. Huang, T. Tan, and Z. Sun, "An iris image synthesis method based on PCA and super-resolution," in *Proc. Int. Conf. Pattern Recognition*, 2004, vol. 4, pp. 471–474.
- [44] L. Ma, T. Tan, Y. Wang, and D. Zhang, "Efficient iris recognition by characterizing key local variations," *IEEE Trans. Image Process.*, vol. 13, no. 6, pp. 739–750, Jun. 2004.
- [45] Z. Sun, Y. Wang, T. Tan, and J. Cui, "Improving iris recognition accuracy via cascaded classifiers," *IEEE Trans. Syst., Man, Cybern. C, Appl. Rev.*, vol. 35, no. 3, pp. 435–441, Aug. 2005.
- [46] D. M. Monro and D. Zhang, "An effective human iris code with low complexity," in *Proc. IEEE Int. Conf. Image Processing*, 2005, vol. 3, pp. 277–280.
- [47] D. M. Monro, S. Rakshit, and D. Zhang, "DCT-based iris recognition," *IEEE Trans. Pattern Anal. Mach. Intell.*, vol. 29, no. 4, pp. 586–595, Apr. 2007.
- [48] D. Taubman and M. Marcellin, *JPEG2000: Image Compression Fundamentals, Standards and Practice*, ser. Kluwer Int. Series in Eng. Comput. Sci. Norwell, MA: Kluwer, 2002.
- [49] K. Gray, "The JPEG2000 standard," presented at the Technische Universität, München, Germany, Feb. 2003.
- [50] M. W. Marcellin, M. J. Gormish, A. Bilgin, and M. P. Boliek, "An overview of JPEG-2000," in *Proc. IEEE Data Compression Conf.*, 2000, pp. 523–541.
- [51] D. Santa-Cruz and T. Ebrahimi, "An analytical study of JPEG 2000 functionalities," in *Proc. IEEE Int. Conf. Image Processing*, 2000, vol. 2, pp. 49–52.
- [52] H. J. Wyatt, "A 'minimum-wear-and-tear' meshwork for the iris," *Vis. Res.*, vol. 40, pp. 2167–2176, 2000.
- [53] D. A. Newsome and I. E. Loewenfeld, "Iris mechanics II: Influence of pupil size on details of iris structure," *Amer. J. Ophthalmol.*, vol. 71, pp. 553–573, 1971.
- [54] "CASIA iris image database" [Online]. Available: <http://www.sinobiometrics.com/>.
- [55] "Kakadu software" [Online]. Available: <http://www.kakadusoftware.com/>.
- [56] L. Ma, T. Tan, Y. Wang, and D. Zhang, "Personal identification based on iris texture analysis," *IEEE Trans. Pattern Anal. Mach. Intell.*, vol. 25, no. 12, pp. 1519–1533, Dec. 2003.
- [57] "Information technology—Iris image interchange format," in *Proc. ANSI/INCITS 379-2004, InterNational Committee for Information Technology Standards*, 2004.
- [58] F. Podio and C. Soutar, "Iris image interchange format," *INCITS—American National Standard for Information Technology*, 2003.



Soumyadip Rakshit (S'04) received the B.Tech. degree in electronics and telecommunications engineering from Kalyani University, Calcutta, India, in 2004.

Currently, he is a Research Student at the University of Bath, Bath, U.K., specializing in iris recognition. His current research interests include biometrics, signal and image processing, pattern recognition, motion estimation, and matching pursuits.



Donald M. Monro (M'92) received the B.A.Sc. and M.A.Sc. degrees from the University of Toronto, Toronto, ON, Canada, in 1964 and 1966, respectively, and the Ph.D. degree at Imperial College, London, U.K., in 1971.

He is Emeritus Professor in Electronic and Electrical Engineering at the University of Bath, Bath, U.K., and Consultant in Signal Processing for biometrics. He spent a brief period in the aeronautical industry. He was Senior Lecturer in Electrical Engineering in 1979 and in the Department of Computing in 1983 at Imperial College, before taking up the Chair of Electronics at The University of Bath in 1991. In addition to biometrics, his research interests are in digital video and audio compression and more general aspects of signal processing.